CARBON PROFILE ANALYSIS OF Fe-Cr-C/Fe-Cr-Ni-C DIFFUSION JOINTS

JIŘÍ SOPOUŠEK[1]*, BOŘIVOJ MILLION[2]

Former experimental observations of Fe-Cr-C/Fe-Cr-Ni-C weldments are compared in this paper with simulated results. The simulation method is based on the CALPHAD approach completed with theory of multi-component bulk diffusion, the local condition of phase equilibria, and assumption that diffusion is the process that controls the rate of phase transformation. The occurred overall carbon concentration peaks near the welded interface are explained by carbide reactions. Both phase and concentration simulated profiles correspond closely to the previous findings. Stable local equilibrium in the diffusion zone and the thermodynamic stability of dissimilar welded joints are discussed.

Key words: weldment, steel, DICTRA, carbon profile, simulation

ANALÝZA UHLÍKOVÝCH PROFILŮ SVAROVÝCH SPOJENÍ Fe-Cr-C/Fe-Cr-Ni-C

Výsledky simulací svarového spojení Fe-Cr-C/Fe-Cr-Ni-C jsou porovnány s dříve získanými experimentálními výsledky. K simulacím je použita metoda CALPHAD doplněná o teorii vícesložkové objemové difuze, o lokální podmínku fázové rovnováhy a o předpoklad, že difuze je řídícím dějem pro rychlost fázové transformace. Pozorované píky celkové koncentrace uhlíku v blízkosti svarového rozhraní jsou vysvětleny karbidickými reakcemi. Simulované fázové a koncentrační profily dobře odpovídají předcházejícím výsledkům. Je diskutováno dodržení podmínky lokální fázové rovnováhy v difuzní zóně a termodynamická stabilita heterogenních svarových spojení.

1. Introduction

Welding joints of dissimilar alloys are technical solutions very frequently used in construction work and advanced material design. The weldability, compatibility, and long-term mechanical/microstructural stability of welded joints are of the

---

[1] Department of Theoretical and Physical Chemistry, Masaryk University, Faculty of Science, Brno, Czech Republic

[2] Institute of Physics of Materials, Academy of Sciences of the Czech Republic, Brno, Czech Republic

* corresponding author, e-mail: `sopousek@chemi.muni.cz`

highest importance [1]. The main factors that influence the stability of a welded joint are the phase nucleation, diffusion, and the rate of phase transformation [2]. These factors depend significantly on temperature. Information on the time evolution of both phase and element redistributions during treatment at particular temperatures is therefore very important.

The microstructure formation in a treated weld joint usually becomes more complicated if a diffusion between two multi-component systems occurs at the joint. In such cases, several mutually influencing phase transformations can be observed [3, 4]. The rate of phase transformations increases substantially if the welded joint is treated at a high temperature [5] because of the temperature dependence of diffusion, the decisive process takes place at higher temperatures. Changes in the chemical potentials of the elements can cause phase precipitation, phase dissolution, and/or phase boundary replacement in the diffusion zone along the welded interface.

Weldments of chromium steel (main components: Fe, Cr, and C) and austenitic stainless steel (main components: Fe, Cr, Ni, and a small amount of C) are simulated in this paper. Samples of the weldments were originally investigated by Bacílek [6]. The majority of these experimental measurements were later subjected to theoretical treatment by Million, Bacílek, and others [7]. They proposed and used a theoretical model that enabled them to evaluate a number of interesting quantities: the carbon effective diffusion coefficient, the carbon activity coefficient, and thermodynamic interaction parameters [7]. They assumed also single-phase carbon diffusion in supersaturated matrices to the left and right of the welded interface, since it was not known how to take into account carbide precipitation and/or dissolution at that time.

In the present work, a second attempt is made to compile all the experimental results presented in [6] using a more progressive theoretical model that enables to incorporate diffusion of all species and carbide reactions occurring in the experimental weldments.

Table 1. Chemical composition (in wt.%) of chromium steels

Steel	C	Mn	Si	P	S	Cr
A	0.30	0.58	0.40	0.028	0.026	0.14
B	0.39	0.91	0.76	0.02	0.018	1.40
C	0.41	0.91	0.76	0.02	0.018	3.40
D	0.48	0.91	0.76	0.02	0.018	6.18
E	0.53	1.13	0.68	0.03	0.020	13.09
F	0.62	1.13	0.68	0.03	0.020	26.82

2. Experimental data

Welded joints of chromium steel with varying composition (see Table 1) and austenitic stainless steel (Table 2) were prepared by Bacílek and Million as described in [6] and [7]. As it can be seen, the chromium steels used (marked by A, B, C, D, E, F) differed mainly in their chromium content. The austenitic stainless steel (marked by St) included Fe, Cr, Ni, and also a small but important amount of carbon. Six steel combinations of weldments were prepared (A|St, B|St, C|St, D|St, E|St, and F|St). Samples from each steel combination were heat-treated under the conditions given in Table 3.

Fortunately, the original samples were available. It enabled to obtain new micrographs of the weldments with higher resolution (e.g. Figs. 1a,b) using light microscopy.

Table 2. Chemical composition (in wt.%) of austenitic stainless steel

C	Mn	Si	P	S	Cr	Ni	Mo	Ti	Al
0.08	1.18	0.39	0.023	0.006	17.91	10.75	0.50	0.45	0.039

Table 3. Heat treatment of weldments

Temperature [°C]	1100	1000	900	800	750	700	650	600	500
Time [h]	1.5	6	16	26.15	37.3	63	112	240	1030

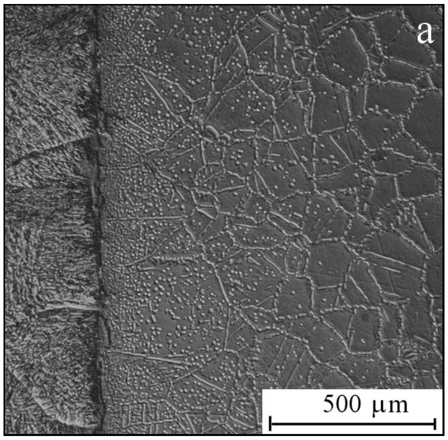

Fig. 1a. Welded joint C/St 900 °C/16 h (Vögels reagent at 90 °C 3 sec/Nital 2 % 10 sec).

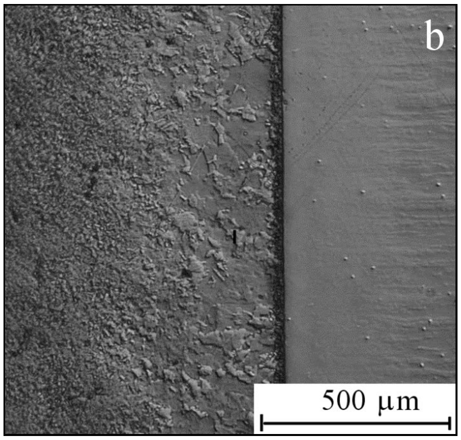

Fig. 1b. Welded joint A/St 650 °C/112 h (Vögels reagent at 90 °C 3 sec/Nital 2 % 10 sec).

3. Simulation model

In the next step, CALPHAD approach was used [8] to assess the composition of phases in equilibrium and also phase diagrams of the investigated alloys. In order to calculate any equilibrium quantity or function (equilibrium composition, chemical potential, activity, etc.), the CALPHAD method requires thermodynamic parameters of the phases. Assessments of these parameters for many systems can be found in the literature, and many programs for such calculations are available now (for example [9] and [10]). However, this approach can only satisfy our need for phase information from areas outside the weldment diffusion zone.

In the case of a heterogeneous weldment, the gradients of chemical potentials usually exist and a diffusion [5] of species occurs. Changes in the chemical potentials of species give the thermodynamic basis for phase transformations, phase precipitation, and/or phase dissolution. This problem studied experimentally in [6] for common weldments can now be solved by considering the multi-component bulk diffusion, local condition of phase equilibria and assuming diffusion as a process controlling the rate of phase transformation [11, 12]. In our study, the DICTRA [13] programme was used to simulate the ageing of the weldments.

The chromium and austenitic steels (see Table 1 and Table 2) involve 7 and 11 elements, respectively. It was found that, taking all elements into account and taking Fe, Cr, Ni, and C as the diffusion species only, the results all fell within the accuracy range of the carbon profile experimental measurements. We therefore used a reduced quaternary base for the Fe-Cr-Ni-C system that had been previously thermodynamically assessed by Hillert and Qui [14]. A similar simplification was done in order to describe diffusion in the experimental weldments. We accepted the data published by B. Jönsson et al. regarding the carbon mobility in bcc [15] and fcc [16], [17] iron lattice.

The experimental weldments were simulated as f.c.c.|f.c.c. or b.c.c.|f.c.c one-dimensional diffusion couples. The major interstitially diffusing element is carbon, but the diffusion of substitutional species (Fe, Cr, Ni) was also considered. In f.c.c. matrix (abr. γ) and b.c.c. matrix (abr. α), carbon and substitutional species (mainly Cr and Fe) form the following carbides: cementite (abr. cem.), M_7C_3 (abr. M7), and $M_{23}C_6$ (abr. M23) [14]. These carbides were treated as non-diffusion spheroid phases [13, 18, 11]. In addition, the diffusion couples b.c.c.|f.c.c were simulated as two interacting cells [13].

4. Result of simulations

The used simulation method enabled us to obtain a substantial amount of information, including temperature-time dependence for many intensive, extensive, and integral quantities. The following time-, temperature-, and distance-dependent quantities were of the highest importance: phase profiles, concentration profiles, activity, and chemical-potential profiles.

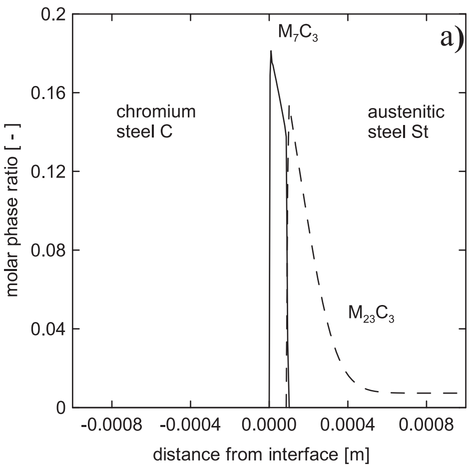

Fig. 2a. Simulated phase profile for C|St weldment at 900 °C after 16 hrs (f.c.c. matrix is the complement phase).

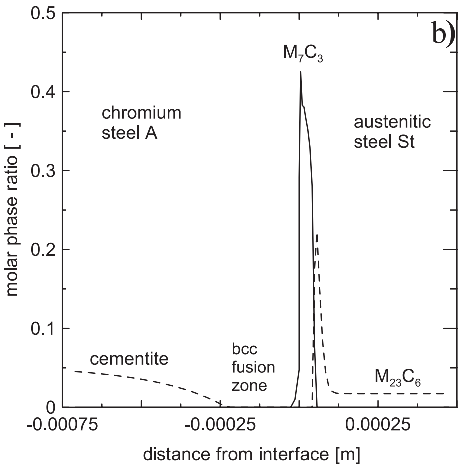

Fig. 2b. Simulated phase profile for A|St weldment at 650 °C after 112 hrs.

Table 4. Significant weldment categories of simulated phase profiles

Weldment description	Label: phase profile record
A high carbon peak in right (chromium steel) from the interface due to carbide precipitation. Both steels with γ matrices.	Ia: γ | (+M7+M23) γ Ib: γ | (+M7+M23) γ+M23
Cementite dissolution in the chromium steel with an α-matrix, and high chromium carbide precipitation in the austenitic steel.	IIa: α+cem.(-cem) | (+M7+M23) γ+M23 IIb: α+cem (-cem+cem+M7) | (-α+M7+M23) γ+α+M23
Weldments with carbide M7 dissolution in the chromium steel with an α-matrix, and high chromium carbide precipitation in right near the interface.	IIIa: α+M7 (-M7) | (+M7+M23) γ+M23 IIIb: α+M7 (-M7) | (+M7+M23) $\gamma + \alpha$+M23
$M_{23}C_6$ carbide redistribution. Dissolution in chromium steel (left), precipitation in the austenitic steel (right).	IV
Negligible carbon diffusion.	V
Transition weldments.	VI

The key information concerning carbide transformations in the weldment are presented as phase profiles (i.e. how depend the matrix and carbide phase ratios on the distance from interface at constant temperatures and times). Examples of

Table 5. Mapping of simulated phase profiles for the investigated weldments (profile records are substituted by labels from Table 4). Numerical values included are: the carbon minimum in chromium steel/the carbon maximum in austenitic steel in wt.% (compare joint C|St in Fig. 3) according to the simulations; corresponding experimental values [6] (in brackets)

Heat treatment	A|St	B|St	C|St	D|St	E|St	F|St
1100 °C/1.5 h	Ia 0.1/0.4 (0.1/0.4)	Ia 0.1/0.6 (0.1/0.4)	Ia 0.2/0.6 (0.1/0.5)	Ia 0.15/0.6 (0.1/0.6)	VI 0.3/0.4 (0.3/0.4)	IV 0.4/0.2 (NA/NA)
1000 °C/3.35 h	Ia 0.1/0.7 (0.0/1.0)	Ia 0.1/1.0 (0.1/0.8)	Ia 0.1/1.0 (0.1/0.9)	Ia 0.2/0.8 (0.2/0.8)	IV 0.2/0.5 (0.0/0.7)	IV 0.2/0.5 (NA/NA)
900 °C/16 h	Ib 0.1/1.0 (0.1/1.1)	Ib 0.1/1.3 (0.1/1.1)	Ib 0.1/1.4 (0.1/1.1)	VI 0.2/1.0 (0.0/1.1)	IV 0.3/0.4 (0.2/0.5)	V – (NA/NA)
800 °C/26.15 h	VI 0.1/2.4 (0.0/2.8)	Ib 0.1/1.7 (0.1/2.2)	VI 0.1/1.6 (0.1/1.7)	VI 0.35/1.4 (0.2/0.9)	IV 0.5/0.4 (0.1/0.4)	V – (NA/NA)
750 °C/37.3 h	VI 0.0/2.5 (0.0/3.7)	VI 0.0/2.3 (0.1/2.8)	VI 0.2/2.0 (0.2/1.6)	VI 0.4/1.0 (0.3/0.9)	IV 0.5/0.4 (0.2/0.2)	V – (NA/NA)
700 °C/63 h	IIa 0.0/3.4 (0.0/3.7)	VI 0.2/2.6 (0.1/2.4)	IIIa 0.2/2.0 (0.2/1.2)	IIIa 0.3/0.8 (0.0/0.4)	IV 0.5/0.25 (NA/NA)	V – (NA/NA)
650 °C/112 h	IIa 0.0/3.1 (0.0/3.1)	VI 0.1/2.6 (0.1/1.6)	IIIa 0.25/1.9 (0.3/0.8)	IIIa 0.4/0.7 (0.3/0.3)	IV 0.5/0.1 (NA/NA)	V – (NA/NA)
600 °C/240 h	IIb 0.0/3.2 (0.0/2.6)	VI 0.2/2.9 (0.2/1.2)	IIIb 0.3/1.8 (0.3/0.5)	IIIb 0.4/0.3 (0.4/0.3)	IV 0.5/0.1 (NA/NA)	V – (NA/NA)
500 °C/1030 h	IIb 0.0/1.3 (0.0/1.1)	VI 0.2/2.2 (0.2/0.5)	IIIb – (0.3/0.3)	IIIb – (NA/NA)	V – (NA/NA)	V – (NA/NA)

the simulated phase profiles are given on Figs. 2a,b. For the sake of simplicity, the simulated phase profile can be written as a corresponding phase record in the following manner (see Table 4): *phase occurrence in the diffusion-unaffected left part of weldment (phase changes in the diffusion-affected left part of the weldment) | (phase changes in the diffusion-affected right part of the weldment) phase occurrence in the diffusion-unaffected right part of the weldment,* where the symbol | stands for the joint interface and where the precipitating (prefix: +) or dissolving (prefix: -) phases in the diffusion zone are shown in brackets. The weldment simulations provided the phase profiles of the weldments. These individual profiles can

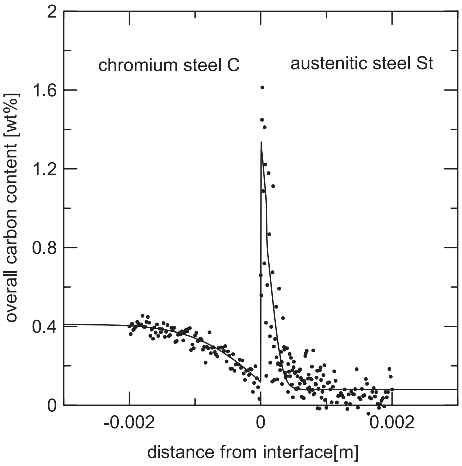

Fig. 3. Experimental and simulated carbon concentration profiles for C/St weldment at 900 ℃ after 16 hrs.

be divided into a few significant categories (Table 4). The phase profile mapping for the investigated weldments is shown in Table 5. The phase ratios as well as the chemical compositions of the phases depend on the distance from the welded interface. They are related to the concentration profiles. The experimental and simulated carbon profiles corresponding to the simulated phase profile from Fig. 2a are given in Fig. 3. It is possible to discern chromium carbide (M_7C_3 and $M_{23}C_6$) precipitation in the diffusion zone.

5. Discussion

A comparison of the experimental [6] and simulated results indicates that the peaks of carbon bulk concentrations (up to 2–3 wt.% C) in the austenitic parts of the weldments can be readily explained by carbide precipitations. A quite satisfactory agreement between the experimental and simulated carbon profiles was found (e.g. Fig. 3). Moreover, the used simulation method enabled us to explain why carbon redistribution was not observed [6] in the F|St weldments. In this case, the simulation proved that there is only a very small difference between carbon activity in F and St alloys despite a big difference in their chemical composition. This means that an F|St weldment is of a high thermodynamic stability at a wide temperature range.

It can be generally stated the used method yields results that reflect quite correctly the phase structure of the weldments. Nevertheless, some topics require further discussion. It was predicted the sequential precipitation of the M_7C_3 and $M_{23}C_6$ carbides occurs in many cases, due to a high carbon activity near the welded interface. This is given by the stable local phase equilibrium condition included in the simulation. The question is if this condition is fulfilled for all diffusion couples.

In the majority of the weldments, it is possible to distinguish between regions having different phase structures (see Figs. 1a,b). In many cases the boundaries of the microstructure regions correspond closely to the simulated phase profiles (compare Fig. 1b and Fig. 2b). However, in some cases the experimental phase-structure regions are wider than the simulated ones (compare Fig. 1a and Fig. 2a). We presume that this reflects greater diffusion of the species due to the grain-boundary diffusion effect.

6. Conclusion

The approach introduced in the present work enabled us to explain the experimental observations of welded joints comprising chromium-rich ferritic and austenitic steels. The peaks of the overall carbon concentration in experimental dependence occurring near the welded interface can be explained by carbide reactions. The simulated phase profiles correspond closely to the experimental findings.

It is necessary to remember an important phenomenon concerning the metastable local phase equilibrium in the diffusion zone. This may be a cause for the absence of the M_7C_3 carbide despite a very powerful stimulus for its precipitation.

The simulation method presented enables to predict the time-evolution of the heat treated heterogeneous welded joints. Using this method of simulation, it is, for example, possible to optimise the chemical compositions of joint materials. It could be very useful in advanced material design when the chemical compositions of the heterogeneous weldments need to be optimised.

Acknowledgements

The funding support provided by the Czech Grant Agency (106/00/0855, 106/01/0382) is gratefully acknowledged. The calculations were performed by ThermoCalc and DICTRA programmes. Sincere thanks are extended to Prof. J. Vřešťál, Dr. M. Svoboda, and to the staff at the Institute of Material Physics of the Academy of Sciences of the Czech Republic.

REFERENCES

[1] PILOUS, V.—STRÁNSKÝ, K.: Structural Stability of Deposits and Welded Joints in Power Engineering. Cambridge, Cambridge Int. Science Publ. 1998.

[2] ÄGREN, J.: In: The Ringberg Workshop 1997 on the Application of Computational Thermodynamics. Calphad, *24,* 2000, p. 15.

[3] SHTANSKY, D. V.—NAKAI, K.—OHMORI, Y.: Z. Metallkd., *90,* 1999, p. 25.

[4] BJÄRBO, A.—HÄTTESTRAND, M.: Metall. Trans., *32A,* 2001, p. 19.

[5] KIRKALDY, J. S.—YOUNG, D. J. : Diffusion in the Condensed State. London, The Institute of Metals 1985.

[6] BACÍLEK, K.: Carbon Redistribution in Heterogeneous Steel Weldments. [Ph. D. Thesis]. Military Academy of Brno 1993.

[7] MILLION, B. et. al.: Z. Metallkd., *86,* 1995, p. 706.

[8] SAUNDERS, N.—MIODOVNIK, A. P.: CALPHAD (Calculation of Phase Diagram) – A Comprehensive Guide (Pergamon Materials Series, Vol. 1). Amsterdam, Elsevier Science 1998.
[9] ThermoCalc (v. M) User's Guide, Div. of Comput. Thermodynamics. Dept. of Mater. Science and Engineering, Royal Inst. of Technology, Stockholm 1997.
[10] PANDAT Software for Multicomponent Phase Diagram Calculation, Madison, Wisconsin USA, CompuTherm LLC 2000.
[11] BORGENSTAM, A.—ENGSTRÖM, A.—HÖGLUND, L.—ÄGREN, J.: J. of Phase Equilibria, *21,* 2000, p. 269.
[12] ANDERSSON, J. O.—HOGLUND, L.—JONSSON, B.—ÄGREN, J.: In: Fundamentals and Applications of Ternary Diffusion. Ed.: Purdy, G. R. New York, Pergamon Press 1990, p. 153.
[13] DICTRA (v. 20) User‘s Guide. Div. of Physical Metallurgy Dept. of Materials Science and Engineering, Royal Inst. of Technology, Stockholm 1998.
[14] HILLERT, M.—QIU, C.: Metall. Trans., *A 22,* 1991, p. 2187.
[15] JÖNSSON, B.: Z. Metallkunde., *85,* 1994, p. 498.
[16] JÖNSSON, B.: Z. Metallkunde., *85,* 1994, p. 502.
[17] JÖNSSON, B.: Z. Metallkunde., *86,* 1995, p. 686.
[18] ENGSTRÖM, A.—HÖGLUND, L.—ÄGREN, J.: Metall. Trans., *A 25,* 1994, p. 1127.

Received: 15.2.2002
Revised: 3.9.2002